10.3.4 Conversion efficiency

Again, we start with the expression for the efficiency

$$\eta = \frac{J_{sc} V_{oc} FF}{P_{in}}. \tag{10.24}$$

Using Eqs. (10.23) and (10.14) and we find

$$\begin{aligned} \eta &= \frac{\eta_{ult} V_{oc} FF}{V_G} (1 - R^*) \mathrm{IQE}^*_{op} \eta^*_G \mathrm{IQE}^*_{el} C_f \\ &= p_{abs} p_{use} (1 - R^*) \mathrm{IQE}^*_{op} \eta^*_G \mathrm{IQE}^*_{el} C_f \eta_V FF, \end{aligned} \tag{10.25}$$

where we used Eqs. (10.9) and (10.10). By filling in the definitions for p_{abs}, p_{use}, η_V and C_f, we obtain [39].

$$\eta = \underbrace{\frac{\int_0^{\lambda_G} \frac{hc}{\lambda} \Phi_{ph,\lambda}\, d\lambda}{\int_0^{\infty} \frac{hc}{\lambda} \Phi_{ph,\lambda}\, d\lambda}}_{1} \underbrace{\frac{E_G \int_0^{\lambda_G} \Phi_{ph,\lambda}\, d\lambda}{\int_0^{\lambda_G} \frac{hc}{\lambda} \Phi_{ph,\lambda}\, d\lambda}}_{2} \underbrace{(1 - R^*)}_{3} \underbrace{\mathrm{IQE}^*_{op} \eta^*_G}_{4} \underbrace{\mathrm{IQE}^*_{el}}_{5} \underbrace{\frac{A_f}{A_{tot}}}_{6} \underbrace{\frac{eV_{oc}}{E_G}}_{7} \underbrace{FF}_{8}. \tag{10.26}$$

This describes the conversion efficiency of a solar cell in terms of components that represent particular losses in energy conversion.

1. Loss due to non-absorption of long wavelengths,
2. Loss due to thermalisation of the excess energy of photons,
3. Loss due to the total reflection,
4. Loss by incomplete absorption due to the finite thickness,
5. Loss due to recombination,
6. Loss by metal electrode coverage, shading losses,
7. Loss due to voltage factor,
8. Loss due to fill factor.

10.4 Design rules for solar cells

Now, as we extensively have discussed all the factors that limit the efficiency of a solar cell we are able to distill three *design rules*. We will use this design rules in Part III when we discuss different PV technologies. The three design rules are

1. Utilisation of the band gap energy,
2. Spectral utilisation,
3. Light management.

We now will take a closer look at each of these design rules.

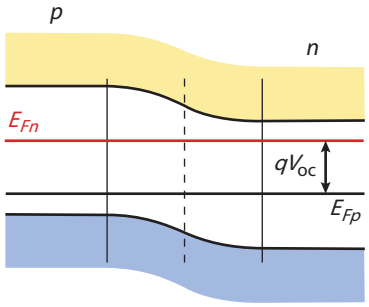

Figure 10.8: The open circuit voltage of a solar cell is determined by the splitting of the quasi-Fermi levels.

10.4.1 Bandgap utilisation

As we have seen earlier in this chapter, the open circuit voltage V_{oc} is always below the voltage V_G corresponding to the bandgap. This loss is characterised with the bandgap utilisation efficiency η_V. The open circuit voltage is determined by the extent to which the quasi-Fermi levels are able to split, which is limited by the charge carrier recombination mechanisms. We discussed the different recombination mechanisms already in detail in Chapter 7. Here, we briefly summarise them and discuss how they affect the bandgap utilisation.

Figure 10.8 shows a p-n-junction, with the p-doped region on the left and the n-doped region right. Further the quasi-Fermi levels are depicted. The extent of splitting between the quasi-Fermi levels determines the open circuit voltage. The open circuit voltage, for example expressed in Eq. (10.17) also can be expressed in terms of the generation rate G_L, the life time τ_0 of the minority charge carriers and the intrinsic density of the charge carriers n_i in the semiconductor material. Under the assumption that G_L is spatially homogenous across the junction, we find

$$V_{oc} \approx \frac{2k_B T}{q} \ln\left(\frac{G_L \tau_0}{n_i}\right). \tag{10.27}$$

The derivation of this equation is out of the scope of this book.

Let us now take a closer look on Eq. (10.27). If we increase the irradiance, or in other words, the generation rate of charge carriers, the open circuit voltage is increased. This is a welcome effect which is utilised in concentrator photovoltaics (CPV), which we will discuss in Section 15.8. Secondly, we see that the lifetime τ_0 plays an important role. The larger the lifetime of the minority charge carrier, the larger the open circuit voltage can be. Or in other words, the longer the lifetime, the larger the possible splitting between the quasi-Fermi levels and the larger the fraction of the bandgap energy that can be utilised.

The lifetime of the minority charge carrier is determined by the recombination rate. As discussed in Chapter 7, we have to consider three different recombination mechanisms: radiative, Shockley-Read-Hall, and Auger recombination. While radiative and Auger recombination depend on the semiconductor itself, SRH recombination is proportional to the density of traps or impurities in the semiconductor. In the three recombination mechanisms energy and momentum are transferred from charge carriers to phonons or photons.

The efficiency of the different recombination processes depends on the nature of the band gap of the used semiconductor material used. We distinguish between *direct* and *indirect* bandgap semiconductors. Crystalline silicon is an indirect band gap material. The radiative recombination in an indirect band gap material is inefficient and recombination will be dominated by the Auger mechanism. For direct band gap materials such as GaAs under moderate illumination conditions, radiative recombination will be the dominant loss mechanism of charge carriers. For very high illumination conditions, Auger recombination starts to play a role as well.

To summarise, we find that in the defect rich solar cells, the open circuit voltage is limited by the SRH recombination. In low-defect solar cells based on indirect band gap materials, the open circuit voltage is limited by Auger recombination. In low-defect solar cells based on direct band gap materials, the open circuit voltage is limited by radiative recombination.

Besides band gap utilisation, it also is important to discuss the relationship between the maximum thickness for the absorber layer of a solar cell and the dominant recombination mechanism. As we have seen in Chapter 7, the recombination mechanism also affects the diffusion length of the minority charge carrier. The diffusion length L_n of minority electrons is given by

$$L_n = \sqrt{D_n \tau_n}, \tag{10.28}$$

where D_n is the diffusion coefficient and τ is the lifetime of the minority charge carrier. Similarly, we can formulate the diffusion length for minority holes, L_p.

It is important to realise that ideally the thickness of the absorber layer should not exceed the diffusion length. In order to understand this requirement, we consider photons that penetrate far into the absorber layer before being absorbed and generating charge carriers. The charge carriers generated deep in the absorber need to diffuse to the *p-n* junction or the back contact for separation and collection. If the distance these charge carriers need to diffuse is exceeding the diffusion length, these excited charge carriers will likely recombine before arriving at the *p-n* junction or back contact. This means that a substantial fraction of the charge carriers generated at a distance larger than the diffusion length from the *p-n* junction or the back contact will not be collected and hence are lost. Only a fraction of the generated carrier density smaller than $1/e$ is collected, where e is the base of the natural logarithm. If the charge carriers are generated within the diffusion length of the *p-n* junction or back contact, the likelihood for collection is much larger. This means that the minority carrier diffusion length limits the maximum thickness of the solar cell.

Mathematically speaking, the influence of the absorber thickness on the V_{oc} is given by

$$V_{oc} \approx C + \frac{k_B T}{q} \cdot \ln\left(\frac{L}{W}\right), \tag{10.29}$$

when the surface recombination velocity is $S = 0$. L is the diffusion length in the absorber, just as above, and W is the thickness (or width) of the absorber. A derivation of this equation is given in Appendix C.

To summarise this section, the open circuit voltage is limited by the dominant recombination mechanism. The dominance of radiative, Auger or Shockley-Reed-Hall recombination depends on the type of semiconductor materials used in the solar cell and the

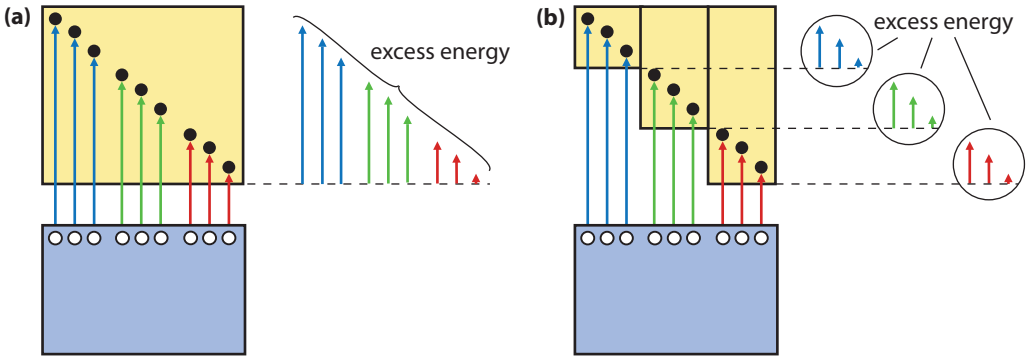

Figure 10.9: Illustrating the lost excess energy in (a) a single-juntion and (b) a multi-junction solar cells.

illumination conditions. We will discuss several different cases on Part III on PV technology.

10.4.2 Spectral utilisation

The spectral utilisation is mainly determined by the choice of materials from which the solar cell is made of. As we have seen in Section 10.2, and mainly Eq. (10.13), the photocurrent density is determined by the bandgap of the material. For a bandgap of 0.62 eV corresponding to a wavelength of 2000 nm, we could theoretically generate a short circuit current density of 62 mA/cm^2. If we consider c-Si, having a band gap of 1.12 eV (1107 nm), we arrive at a theoretical current density of 44 mA/cm^2.

The optimal bandgap for single-junction solar cells is determined by the Shockley-Queisser limit, as illustrated in Fig. 10.6. For single junction solar cells, semiconductor materials such as silicon, gallium arsenide and cadmium telluride have a band gap close to the optimum.

In Part III we will discuss various concepts that allow to surpass the Shockley-Queisser limit. Here, we will briefly discuss the concept of *multi-junction solar cells*. In this devices, solar cells with different bandgaps are stacked on top of each other. As illustrated in 10.9, the excess energy can be reduced significantly, and the spectral utilisation will improve.

10.4.3 Light management

The third and last design rule that we discuss is *light management*. In an ideal solar cell, all light that is incident on the solar cell should be absorbed in the absorber layer. As we have discussed in Section 4.4, the intensity of light decreases exponentially as it travels through an absorptive medium. This is described by the Lambert-Beer law that we formulated in Eq. (4.25),

$$I(d) = I_0 \exp(-\alpha d). \tag{10.30}$$

From the Lambert-Beer law it follows that at the side, at which the light is entering the film, more light is absorbed in reference to the back side. The total fraction of the incident light